J HK Coll Radiol 2003;6:36-39

CASE REPORT

Computed Tomographic Diagnosis of Unsuspected Pericarditis

RT Dwyer, T Khalil

Department of Radiology, Westmead Hospital, Westmead, New South Wales, Australia

ABSTRACT

There is a paucity of scientific literature regarding the utility of computed tomography in the diagnosis of acute pericarditis. This report may be the first in the English language literature to document a diagnosis of clinically unsuspected acute pericarditis made using computed tomography. Spiral computed tomography has the capacity to diagnose acute pericarditis, since lymphadenopathy and hazing of the epicardial and mediastinal fat planes may be diagnostic signs for this pathology.

Key words: *Computed tomography, Fibrosis, Inflammation, Pericarditis*

INTRODUCTION

Computed tomography (CT) is widely used in the assessment of acute intrathoracic pathology. The role of CT in the investigation of thoracic aortic injury, acute aortic dissection, pulmonary thromboembolic (PTE) disease, pulmonary laceration, and skeletal injury is well established. In contrast to other modalities (catheter angiography, and echocardiography and lung scintigraphy), CT is frequently able to assess multiple pathologies in different organs and diagnose pathology not clinically suspected. In the investigation of acute chest pain, the use of CT has been limited mainly to assessment of aortic pathology and PTE disease. Pericardial diseases may be difficult to diagnose clinically, mimicking cardiac and other intrathoracic pathology.[1] This report is of a patient in whom spiral CT of the thorax identified unsuspected pericarditis as the cause of acute chest pain.

CASE REPORT

A 68-year-old man presented with a 1-week history of intermittent dull central chest pain, radiating to the back and occasionally to the left shoulder. On the day of presentation, the pain worsened dramatically, and developed a pleuritic component. Past medical history included admission to hospital 1 year previously with faecal peritonitis secondary to ileal loop perforation. The ileal loop had infarcted from a closed loop obstruction caused by adhesions, following surgery for para-umbilical hernia repair. Post-laparotomy progress was complicated by lower limb deep venous thrombosis and sub-phrenic collections from which methicillin-resistant *Staphylococcus aureas* (MRSA) and acinetobacter were isolated. Other past surgical history included the insertion of a ventriculo-peritoneal shunt following cerebral arachnoid cyst removal, cervical laminectomy, and traumatic amputation of the left hand. Comorbidities included chronic obstructive pulmonary disease, systemic hypertension, type II diabetes, and atrial fibrillation. Medications included nebulised salbutamol and ipratropium bromide, digoxin, enalapril, warfarin, glibenclamide, frusemide, potassium, and calcium supplements. The patient was born in Jamaica and had lived in Guam before migrating to Australia in 1974. He had ceased smoking 15 years previously, and had no known allergies.

On examination, blood pressure was 80/40 mm Hg, with a systolic pressure of 120 mm Hg after fluid resuscitation. The patient was afebrile, pale, and dyspnoeic. Pulse was regular at 60 beats per minute, although weak, but there was no pulsus paradoxus. Jugular venous pressure was not raised and heart sounds were dual but soft. There were coarse crepitations throughout both lung fields. Electrocardiography showed left bundle branch block. The chest radiograph was normal, with no mediastinal widening.

Correspondence: *Dr R Dwyer, Department of Radiology, Westmead Hospital, Westmead, NSW 2145, Australia.*
Tel: (612) 9845 6522; Fax: (612) 9687 2109;
E-mail: rrdw@imag.wsahs.nsw.gov.au

Submitted: 20 November 2002; Accepted: 24 January 2003.

The provisional diagnosis was acute aortic dissection. Unstable angina, myocardial infarction, and pulmonary embolic disease were the differential diagnoses considered. Single detector spiral thoracic CT scanning was performed using a Siemens Plus 4 unit (Siemens, Erlanger, Germany). Pre-contrast 8 mm axial sections from the aortic root to the aortic arch were obtained. After intravenous administration of 100 ml Iomeron 300 (Bracco spa, Milan, Italy) at a rate of 4 ml/second, contiguous axial 8 mm section scans were taken in the arterial phase, from 20 mm above the aortic arch to the common iliac arteries. Scan parameters were: voltage120 kV, tube current 220 mA on pitch of 2, with tube rotation time 0.75 seconds/360°. Images were printed on mediastinal settings (window = 450; level = 50), and parenchymal settings (window = 1650; level = -300). There was no evidence of aortic dissection. A moderate-sized pericardial effusion was seen, with hazing of epicardial and mediastinal fat (Figures 1 and 2). Subtle reactive mediastinal lymphadenopathy was noted (Figure 2). A CT diagnosis of acute pericarditis was made on the basis of these findings.

Transthoracic echocardiography following CT confirmed the pericardial effusion, maximum thickness 15 mm. Right atrial pressure was elevated and the right heart contour flattened, consistent with tamponade. Pericardiocentesis yielded 150 ml of cloudy yellow fluid, with slight blood staining. Ventilation perfusion lung scanning indicated a low probability of PTE disease. The patient commenced empirical therapy of vancomycin and imipenem in view of the previously cultured MRSA and acinetobacter. The pericardial fluid extracted was shown to be an acute inflammatory exudate, with 21.1 $x10^9$/L white cells (predominantly neutrophils), and a protein level of 7.1 g/L with no organisms seen, no culture growth after 5 days, and no malignant cells. An initial complete blood count showed leukocytosis, with a white cell count of 12.4 $x10^9$/L (normal range, 4.5-11.0 $x10^9$/L) and neutrophilia (81%). The erythrocyte sedimentation rate was 82 mm/hour (normal range, 0 to 20 mm/hour) and the international normalised ratio was 0.9 at admission. Liver function tests, cardiac enzymes, and serum electrolytes remained normal throughout admission. Hepatitis B and C serology were negative.

An infectious diseases consultant considered that acute bacterial pericarditis was unlikely since all cultures were negative. In view of the patient's prior residency in Guam, tuberculosis was considered and Mantoux testing suggested but not performed. Antibiotic therapy was discontinued.

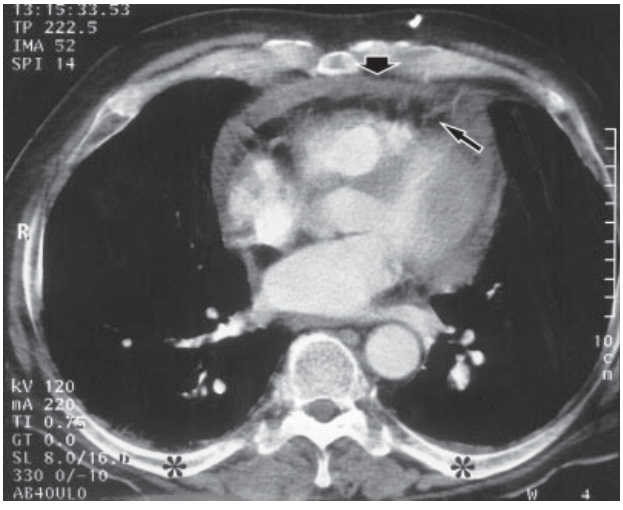

Figure 1. Spiral thoracic post-contrast computed tomography scan at the level of the superior pulmonary vein entrance to the left atrium. An effusion of 10 mm maximum thickness (thick arrow) is seen, with stranding of the epicardial fat (thin arrow). Similar, although less pronounced, features are seen in the adjacent ventral mediastinal fat. Small bi-basal pleural effusions are seen immediately anterior to the ribs (asterisks). The subcutaneous fat planes are normal in appearance.

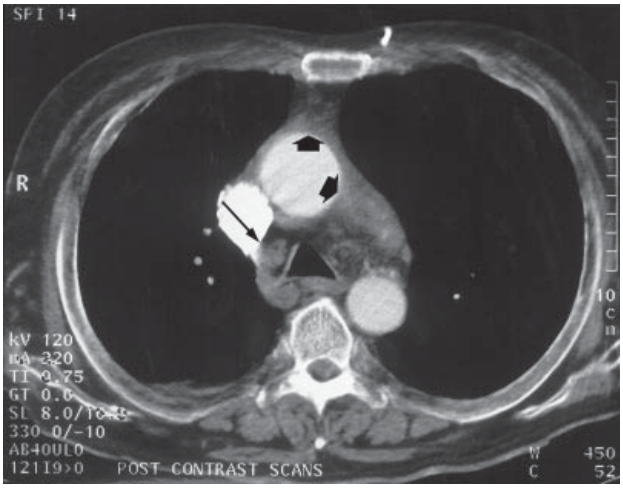

Figure 2. Spiral thoracic post-contrast computed tomography scan at the level of the aortopulmonary window. The aortopulmonary window and the pre-aortic mediastinal fat planes (thick arrows) appear hazed. The right paratracheal lymph node short axis is 10 to 12 mm (thin arrow). A number of small round sub-centimetre densities in the left paratracheal space can be seen. These may represent non-enlarged nodes.

Progress echocardiography on day 11 after admission showed re-accumulation of pericardial fluid. A left mini-thoracotomy with formation of a pericardial window was performed 12 days after admission. The epicardial layer of the pericardial sac was covered with dark red cortex, and there was an exudate on the myocardial surface.

The pericardium was markedly thickened, oedematous, and inflamed. Pericardial biopsy for histopathology and tissue culture was taken, with 300 ml of straw-coloured fluid drained.

Investigation of pericardial fluid again demonstrated inflammatory exudate. Macroscopic pathology showed a congested, haemorrhagic, and necrotic pericardial specimen. Histopathology reported a markedly fibrotic, haemorrhagic and thickened (4 mm) pericardium with chronic inflammation and granulation tissue beneath a superficial layer of fibrin. There were no granulomata, atypical, or malignant cells seen. The final pathological diagnosis was "fibrosis and chronic inflammation". The patient's clinical condition improved and he was discharged 19 days after admission, with no aetiology for the pericarditis established.

DISCUSSION

This patient is the first for whom CT has prospectively diagnosed unsuspected pericarditis. The course of subsequent investigation and management were dictated by this imaging result. Fat hazing and lymphadenitis were critical CT signs in diagnosing an acute component to the pericarditis. Pericardial histopathology revealed fibrosis and chronic pericarditis only. However, this biopsy was collected 12 days following presentation and the commencement of treatment. It did not include epicardial or adjacent mediastinal fat, where the critical CT features were observed. Abnormalities consistent with inflammation at the epicardial fat surface of the pericardium were documented at thoracotomy, correlating with CT findings. Exudative effusion is uncommon in pure chronic pericarditis. Clinical features also suggested an acute component to the process, supported by early laboratory results of systemic and pericardial fluid neutrophilia. It is likely that the presenting illness and CT findings reflected acute-on-chronic pericarditis.

In the pre-spiral CT era, CT became an established modality for assessing paracardiac masses, pericardial thickening, calcification, and loculated pericardial collection.[2] Echocardiography has been considered more efficacious than CT in evaluating uncomplicated pericardial effusions, particularly those of small volume.[3,4] Pericardial thickening,[5,6] lobulation,[7] gas locules,[8] and contrast enhancement[3,9] are recognised CT indicators of acute pericarditis. Previous reports have not described fat hazing and lymphadenopathy as associated signs, even in experimental models.[9] This may reflect greater slice acquisition time (2 to 5 seconds), and slice thickness in non-spiral technology, causing cardiac motion artefact,[10] and partial volume averaging. Non-spiral CT thorax studies have been routinely undertaken with 10 mm slice thickness. For multidetector thoracic CT workstation reporting, 1 to 3 mm sections are commonly recorded for studies requiring high spatial resolution.[11]

Increasing scan speed, and decreasing reconstruction slice thickness, have created new opportunities for cardiac and paracardiac imaging. The dense 1 to 2 mm thick line of normal pericardium is usually well-delineated by CT. It is composed of an outer thick fibrous layer, and a thin double-layered serosa. The outer serosal layer, the parietal pericardium, and the inner layer, the visceral pericardium, are separated by a thin lubricating quantity of fluid.[12] Pericardial effusion accumulates between the 2 serosal layers. The parietal serous pericardium is attached to the fibrous pericardium. Delineation of the pericardium on CT is aided by the tissue planes on its internal and external aspects. Pericardium contacts mediastinal fat and pleura[13] and the lungs at its external aspect. Internally, the visceral layer of the serosal pericardium is separated from myocardium by subepicardial fat.[14] This case suggests that inspection of this fat plane is important for detecting acute pericardial pathology.

There are potential pitfalls in assessing epicardial fat and lymph nodes that could lead to the false positive diagnosis of acute pericarditis. Systemic processes, such as disturbed oncotic pressure and septic shock, may cause widespread oedema of the fat planes and thickening of their fibrous septa. The presence of normal non-mediastinal fat structures should thus be confirmed before inferring pericardial disease on the basis of epicardial fat findings.

The use of CT is notoriously unreliable for assessing lymph node pathology. Glazer et al suggested that an arbitrary short axis node measurement of no greater than 10 mm should be used to define mediastinal lymphadenopathy, despite the variable size distribution of normal nodes in the mediastinum.[15] Altering this measurement in either direction has deleterious effects on CT sensitivity or specificity for lymphadenopathy. In the patient presented, 10 and 12 mm short axis nodes were seen, and this was inferred as representing lymphadenitis. The sub-centimetre left paratracheal nodes do not satisfy Glazer et al's criteria for lymphadenopathy.[15] However, using size criteria alone

excludes consideration of the number of nodes in a region, or other relevant CT findings such as fat plane pathology. Morphological assessment of nodes by CT is likely to remain unsatisfactory. The development of functional contrast agents may improve the utility of CT in lymph node evaluation. Although pericardial fluid density assessment has been used to characterise serous, exudative, chylous, and haemorrhagic effusions,[16-18] this parameter was not evaluated in this patient.

CONCLUSION

Developments in spiral CT technology have progressively decreased cardiac motion artefact, and have allowed reductions in image slice thickness. Pathology involving epicardial and mediastinal fat may be more sensitively detected than in the pre-spiral CT era. Hazing and stranding of these structures, and the presence of lymphadenopathy may be important ancillary signs of acute pericarditis. However, the sensitivity and specificity of these signs remain to be validated.

REFERENCES

1. Schiavone WA, Rice TW. Pericardial disease: current diagnosis and management methods. Cleve Clin J Med 1989;56: 639-645.
2. Lackner K. Value and limitations of computed tomography of the heart. Eur J Radiol 1985;5:158-165.
3. Olson MC, Posniak HV, McDonald V, Wisniewski R, Moncada R. Computed tomography and magnetic resonance imaging of the pericardium. Radiographics 1989;9:633-649.
4. Solomon A, Weiss J, Stern D, Barmeir E. Computerized tomography in pericardial disease. Heart Lung 1983;12:513-515.
5. Sato TT, Geary RL, Ashbaugh DG, Jurkovich GJ. Diagnosis and management of pericardial abscess in trauma patients. Am J Surg 1993;165:637-642.
6. Jeffrey RB, Webb WR. CT appearance of rheumatoid pericarditis. J Comput Assist Tomogr 1980;4:866-868.
7. Tabrizi SJ. Grand Rounds Hammersmith Hospital: nocardia pericarditis. BMJ 1994;309:1495-1497.
8. Ivey MJ, Gross BH. Back pain in an elderly patient. Chest 1993; 103:1851-1853.
9. Hackney D, Slutsky R, Mattrey R, et al. Experimental pericardial inflammation evaluated by computed tomography. Radiology 1984;151:145-148.
10. Cordes D, DeGroff C, Shaffer EM. Spontaneous pericardial haematoma in an infant. Pediatr Cardiol 1999;20:380-381.
11. Remy-Jardin M, Remy J, Baghaie F, Fribourg M, Artaud D, Duhamel A. Clinical value of thin collimation in the diagnostic workup of pulmonary embolism. AJR Am J Roentgenol 2000;175: 407-411.
12. Williams PL, Warwick R, editors. Gray's anatomy. Edinburgh: Churchill Livingstone; 1980.
13. Moncada R, Kotler MN, Churchill RJ, Demos TC, Jacobs W, Steiner RM. Multimodality approach to pericardial imaging. Cardiovasc Clin 1986;17:409-441.
14. Isner JM, Carter BL, Bankoff MS, Konstam MA, Salem DN. Computed tomography in the diagnosis of pericardial heart disease. Ann Intern Med 1982;97:473-479.
15. Glazer GM, Gross BH, Quint LE, Francis IR, Bookstein FL, Orringer MB. Normal mediastinal lymph nodes: number and size according to American Thoracic Society mapping. AJR Am J Roentgenol 1985;145:261-265.
16. Starling RC, Yu VL, Shillington D, Galgiani J. Pneumococcal pericarditis: Diagnostic usefulness of counterimmunoelectrophoresis and computed tomographic scanning. Arch Intern Med 1986;146:1174-1176.
17. Tomoda H, Hoshiai M, Furuya H, et al. Evaluation of pericardial effusion with computed tomography. Am Heart J 1980;99: 701-706.
18. Moncada R, Baker M, Salinas M, et al. Diagnostic role of computed tomography in pericardial heart disease: congenital defects, thickening, neoplasms and effusions. Am Heart J 1982;103: 263-282.